

Host galaxy and orientation differences between different AGN types

Anamaria Gkini^{1,2}, Manolis Plionis^{3,4}, Maria Chira^{2,4} and Elias Koulouridis²

¹ Department of Astrophysics, Astronomy & Mechanics, Faculty of Physics, National and Kapodistrian University of Athens, Panepistimiopolis Zografou, Athens 15784, Greece

² Institute of Astronomy, Astrophysics, Space Applications and remote Sensing, National Observatory of Athens, GR-15236 Palaia Pendeli, Greece

³ National Observatory of Athens, GR-18100 Thessio, Athens, Greece

⁴ Sector of Astrophysics, Astronomy & Mechanics, Department of Physics, Aristotle University of Thessaloniki, Thessaloniki 54124, Greece

September 3, 2021

ABSTRACT

Aims. The main purpose of this study is to investigate aspects regarding the validity of the active galactic nucleus (AGN) unification paradigm (UP). In particular, we focus on the AGN host galaxies, which according to the UP should show no systematic differences depending on the AGN classification.

Methods. For the purpose of this study, we used (a) the spectroscopic Sloan Digital Sky Survey (SDSS) Data Release (DR) 14 catalogue, in order to select and classify AGNs using emission line diagnostics, up to a redshift of $z = 0.2$, and (b) the Galaxy Zoo Project catalogue, which classifies SDSS galaxies in two broad Hubble types: spirals and ellipticals.

Results. We find that the fraction of type 1 Seyfert nuclei (Sy1) hosted in elliptical galaxies is significantly larger than the corresponding fraction of any other AGN type, while there is a gradient of increasing spiral-hosts from Sy1 to LINER, type 2 Seyferts (Sy2) and composite nuclei. These findings cannot be interpreted within the simple unified model, but possibly by a co-evolution scheme for supermassive black holes (SMBH) and galactic bulges.

Furthermore, for the case of spiral host galaxies we find the Sy1 population to be strongly skewed towards face-on configurations, while the corresponding Sy2 population range in all host galaxy orientation configurations has a similar, but not identical, orientation distribution to star-forming (SF) galaxies. These results also cannot be interpreted by the standard unification paradigm, but point towards a significant contribution of the galactic disc to the obscuration of the nuclear region. This is also consistent with the observed preference of Sy1 nuclei to be hosted by ellipticals, that is, the dusty disc of spiral hosts contributes to the obscuration of the broad-line region (BLR), and thus relatively more ellipticals are expected to appear hosting Sy1 nuclei.

Key words. galaxies: Seyfert - galaxies: active - galaxies: nuclei - galaxies: evolution - galaxies: bulges - galaxies: statistics

1. Introduction

The unification model of active galactic nucleus (AGN) explains the wide variety of features discerned in different classes of AGN in terms of the anisotropic geometry of the black hole's immediate surroundings (e.g. Antonucci 1993; Urry & Padovani 1995; Netzer 2015)). It is well known that AGNs have a central supermassive black hole (SMBH) that accretes surrounding matter, and a toroidal structure by dust molecular gas that absorbs a fraction of the emitted radiation. Near the SMBH, the high-speed gas clouds produce the broad-line region (BLR), while far away from this the torus clouds that move at low speeds produce the narrow-line region (NLR). In the simplest form of the unification paradigm (UP), the observed differences between type 1 Seyfert (Sy1) and type 2 Seyfert (Sy2) objects are due to orientation effects with respect to the line of sight to the observer.

An important implication of this simple model is that, since the observed differences between AGN types are attributed solely to orientation effects, the host galaxies of AGN should be intrinsically the same (e.g. Netzer 2015; Hickox & Alexander 2018). Thus, despite their success in explaining a range of AGN observed features, such as the absence of broad-line features in the spectra of Sy2 galaxies, it has become clear that the simplest

models of unification are inconsistent with observations and cannot explain aspects such as the lack of Sy1s in isolated pairs of galaxies (González et al. 2008) and in compact groups (Martínez et al. 2008; Bitsakis et al. 2010), the lack of hidden BLRs in many Sy2 AGNs in polarised spectra (Tran 2001, 2003), and the absence of detected BLRs in low-accretion-rate AGNs (e.g. Nicastro et al. 2003; Elitzur & Ho 2009). Specifically, according to studies investigating the differences between Sy1s and Sy2s (e.g. Keel 1980; Kinney et al. 2000; Koulouridis et al. 2006; Rigby et al. 2006; Martínez-Sansigre et al. 2006a; Lacy et al. 2007; Lagos et al. 2011; Ramos Almeida et al. 2011; Elitzur 2012; Villarroel et al. 2012; Koulouridis 2014; Villarroel & Korn 2014; Netzer 2015; Villarroel et al. 2017; Bornancini & García Lambas 2018; Zou et al. 2019; Yang et al. 2019; Bornancini & García Lambas 2020; Malizia et al. 2020) and the connection with their host galaxies at redshifts $0.03 < z < 0.2$ (e.g. Villarroel et al. 2012; Koulouridis et al. 2013; Villarroel & Korn 2014), it has been shown that type 1 and type 2 Seyfert galaxies have different optical, mid-infrared, X-ray, and morphological properties (e.g. Sorrentino et al. 2006; Slavcheva-Mihova & Mihov 2011; Villarroel et al. 2017; Chen & Hwang 2017; Bornancini & García Lambas 2018), and they also reside in statistically dif-

ferent environments (e.g. Koulouridis et al. 2013; Villarroel & Korn 2014; Jiang et al. 2016; Bornancini et al. 2017; Bornancini & García Lambas 2018, 2020). In particular, Bornancini & García Lambas (2020) showed that the ultraviolet (UV), optical, and mid-infrared (IR) colour distribution of the different AGN classes differ significantly, while Villarroel & Korn (2014) found that the activity and colour between the neighbours of Sy1s and Sy2s are significantly different, and that the spiral fraction of the host galaxies depends on the environment of Sy1 and Sy2 galaxies in different ways. Moreover, it is found that the neighbours of Sy2 AGN are more star-forming and bluer than Sy1 AGNs (see also Koulouridis et al. 2013) and also that Sy2 hosts are surrounded by a larger number of dwarf galaxies (Villarroel et al. 2012). Additionally, the morphology of Sy1 galaxies shows no indications of close interactions, which means either that they rarely merge (Koulouridis 2014), or that they are extremely short-lived AGNs (Villarroel et al. 2012). Bornancini & García Lambas (2018) find that Sy2s have more abundant neighbours at high redshifts ($0.3 < z < 1.1$) and that Sy1 hosts are preferably elliptical or compact galaxies, while Sy2 hosts present a broader Hubble-type distribution.

Many studies (e.g. Ramos Almeida et al. 2011; Elitzur 2012; Villarroel et al. 2017; Suh et al. 2019) reveal that differences between the two types of AGN also lie in the star formation rate (SFR), in the structure of the torus and the physics of the central engines. Most notably, Suh et al. (2019) and Villarroel et al. (2017) found that the two Seyfert populations have different luminosities with Villarroel et al. (2017) supporting that type 1 AGNs are ten times more luminous than type 2s. Suh et al. (2019) also concluded that Sy1 and Sy2 host galaxies seem to have different SFRs, while Villarroel et al. (2017) detected many more supernovae (SNe) in type 2 AGN hosts, which implies differences between stellar ages and more recent star formation in Sy2 hosts. On the other hand, Bornancini & García Lambas (2018) found no difference between the SFR distribution of tracer galaxies in both AGN samples at larger scales ($r_p < 500$ kpc). In addition, in the context of differences in the structural features of the torus, Ramos Almeida et al. (2011) found that the Sy2 torus is broader and has more clouds than that of Sy1 and that the optical depth of the clouds in Sy1 torus is larger than in Sy2. They suggest that the type 1/type 2 classification depends on the torus intrinsic properties rather than in the torus inclination (e.g. Elitzur 2012; Audibert et al. 2017). Previous work (e.g. Mendoza-Castrejón et al. 2015) has also claimed that the Sy1 and Sy2 active nuclei have different torus clumpiness, while they also found a dependence on whether the host is in a merger or isolated.

Since, observations do not fully comply with the predictions of the simple ‘*A type 2 AGN is just a type 1 AGN viewed through a dust*’ model, alternative or complementary factors affecting the observed AGN types should be sought in order to explain the AGN variety. Indeed, Koulouridis et al. (2006) and Jiang et al. (2016), when studying the environments of Sy1 and Sy2 galaxies at low redshifts, found that both AGN classes have similar clustering properties (e.g. Zou et al. 2019), but at scales smaller than $100kpc$ Sy2s have significantly more neighbours than Sy1s (e.g. Bornancini & García Lambas 2018). These results contrast with those of Melnyk et al. (2018), who obtained similar local- and large-scale environments for the different AGN types. Jiang et al. (2016) also found significant differences in the infrared colour distributions of the host galaxies of the two AGN types. Besides this, Powell et al. (2018) reported that nearby type 2 AGNs reside in more massive halos than type 1s, which is un-

like the results of Jiang et al. (2016), who found that their halo masses are similar.

Furthermore, some studies (e.g. Keel 1980; Maiolino & Rieke 1995; McLeod & Rieke 1995; Malkan et al. 1998; Matt 2000; Schmitt et al. 2001; Martínez-Sansigre et al. 2006a; Rigby et al. 2006; Lacy et al. 2007; Lagos et al. 2011; Goulding et al. 2012; Netzer 2015; Burtscher et al. 2016; Jiang et al. 2016; Buchner & Bauer 2017; Lanzuisi et al. 2017; Bornancini & García Lambas 2018; Zou et al. 2019; Malizia et al. 2020; Masoura et al. 2021) claim that the host galaxy might have a non-negligible contribution to the optical obscuration of nuclei. For example, He et al. (2018) suggest that obscuration on both circum-nuclear ($\sim pc$) and galactic ($\sim kpc$) scales are important in shaping and orienting the AGN narrow-line regions. Further evidence comes from high-resolution observations, in nearby type 2 AGNs, which have revealed that the nucleus is covered by a large-scale – a few hundred pc – dust filament or diffuse dust lane (Prieto et al. 2014). Moreover, Chen et al. (2015) found that the obscuration at X-ray and optical bands in type 2 quasars is connected to the far-IR-emitting dust clouds usually located on the scale of the host galaxy. Furthermore, Malizia et al. (2020) recently published an analysis using a hard X-ray-selected AGN sample showing that material located in the host galaxy on scales of hundreds of parsec, while not aligned with the absorbing torus, can be extended enough to hide the BLR of some Sy1s causing their misclassification as Sy2 objects and giving rise to the deficiency of around 24% of Sy1s in edge-on galaxies.

The different average AGN luminosities and stellar ages of the host galaxies of the Sy1 and Sy2 populations could be explained within the framework of an evolutionary scenario. According to Koulouridis et al. (2006) and Krongold et al. (2002), in some cases the interaction between gas-rich galaxies ignites starburst activity, while large amounts of gas and dust obscure the central nuclear region at this stage. As the starburst dies off, the remaining molecular gas and dust forms a torus around the disc and eventually the AGN will attenuate the obscuring medium. Namely, this model proposes an AGN evolutionary sequence going from starburst to type 2, and finally to type 1, Seyfert galaxies (e.g. Springel et al. 2005; Hopkins et al. 2006; Koulouridis et al. 2013; Elitzur et al. 2014; Villarroel & Korn 2014; Mendoza-Castrejón et al. 2015; DiPompeo et al. 2017a; Yang et al. 2019; Spinoglio & Fernández-Ontiveros 2019).

Studies in polarised light to Sy2 galaxies have shown that in many low-luminosity AGN the dusty torus is absent, while the BLR is also not detected (e.g. Elitzur & Shlosman 2006; Perlman et al. 2007; Trump et al. 2011; Koulouridis 2014; Hernández-Ibarra et al. 2016). These results are consistent with those of Trump et al. (2011), who support the notion that above a specific accretion rate ($(L/L_{Edd} \gtrsim 0.01)$) AGNs can be observed as broad-line or as obscured narrow-line AGNs, while for $(L/L_{Edd} \lesssim 0.01)$ the BLR becomes non-detectable. Additionally, the obscuring torus tends to become weaker or disappears (Elitzur et al. 2014).

The above findings could be incorporated within the evolutionary scheme. If the accretion-rate-dependent scenario is valid, one would expect that AGNs could lose their torus or/and their BLR at the end of the AGN duty cycle, as the accretion rate drops below a critical value (e.g. Elitzur & Ho 2009; Elitzur et al. 2014; Koulouridis 2014). This implies that firstly, AGNs can appear as type 1, after the quenching of the star-forming activity by the AGN feedback and the disappearance of the torus (Krongold et al. 2002) and secondly, these type 1s will evolve to true type 2 AGNs due to the elimination of the BLR, based, for example, on the wind-disc scenario of Elitzur & Ho (2009).

In summary, the plethora of results of many relevant studies clearly indicate that the viewing angle alone cannot fully account for the different AGN types. It is within this ideology that the current study lies, investigating the orientation properties of spiral hosts, as well as the Hubble-type distribution of different types of AGNs.

After the presentation of the data used in Sect. 2, the main body of our analysis is organised as follows. In Sect. 3.1, we study the morphology frequency distribution of host galaxies for different AGN types comparing to that of the non-active star-forming sample, after statistically matching their respective redshift distribution in order to suppress possible evolutionary effects. In Sect. 3.2, we study the frequency distribution of spiral host galaxy orientations (b/a) for the Sy1 and Sy2 sub-samples, comparing with that of non-active star-forming (SF) galaxies (which we use as a control sample). We only used galaxies with high 'spirality' probability > 0.8 (as defined by the Galaxy Zoo project), also statistically matching their respective redshifts and stellar mass distributions.

2. Observational data

For the purposes of the current study, we used galaxy catalogues extracted from the Sloan Digital Sky Survey (SDSS) Data Release (DR) 14 (Abolfathi et al. 2018) in five bands (u,g,r,i,z) with a magnitude limit for the spectroscopic sample of $m_r = 17.77$ in the r-band, in order to have a homogeneous magnitude cut-off over the largest possible SDSS area. Our catalogues consist of 3.800 Sy1, 56.846 Sy2, 120.025 Composite, 107.034 LINER, and 263.223 SF galaxies with redshift $z < 0.2$. The above classifications are derived from the spectroscopic reanalysis by the MPA-JHU teams of a large sub-sample of SDSS galaxies, as described in Tremonti et al. (2004) and Brinchmann et al. (2004). The morphology characterisation of the galaxies is based on the Galaxy Zoo Project (Lintott et al. 2008), a crowd-sourced astronomy project that asks citizens to characterise galaxies as spirals or ellipticals and to determine the rotation direction of spirals by inspecting SDSS galaxy images (Raddick et al. 2007). In order to ensure the reliable classification of our galaxies, we performed a quality cut on our catalogue, rejecting galaxies with H α rest-frame equivalent width (EW) $< 8 \text{ \AA}$, which, although it is a rather arbitrary limit, we verified to be adequately secure via an inspection of a sufficiently large sub-sample.

The Sy1 sample (see Appendix) comprises all galaxies with a Balmer line width of σ greater than 500 km/sec (FWHM > 1180 km/s). We note that in the SDSS database all such sources are catalogued with $\sigma = 500$ km/sec, while this is actually a lower limit. Visual inspection of a large number of spectra validated that these sources are bona fide broad-line Seyferts. All spectra with an emission line of $\sigma > 200$ km/sec are also characterised as broad line in the SDSS database. We visually reviewed all spectra in our spiral galaxy sample that fall in this category (450 sources), and we conclude that they contain very few that could be unambiguously classified as broad-line AGNs. Therefore, to reduce noise in our analysis, we chose to exclude all spectra with Balmer lines of $\sigma < 500$ km/sec from our Sy1 sample.

After the above procedures, our final sample of secure objects consists of 1.378 Sy1, 7.498 Sy2, 26.544 Composite, 1.926 LINER, and 203.298 SF galaxies.

The classification between different type of narrow-line AGNs and SF galaxies has been performed utilising the BPT diagram classification method of Baldwin et al. (1981).

It is important to note that we will use the SF galaxies, of which the vast majority are spirals, as our control sample since

their disc orientations cover the whole range of viewing angles with respect to the line of sight. Additionally, they are mainly non-AGN galaxies, and even when hosting an AGN in their centres the star formation dominates the emission. This leads to spectra characteristic of non-AGN galaxies (Siebenmorgen et al. 2015).

Before proceeding, we felt it necessary to investigate the level of consistency between the morphology classification of the Galaxy Zoo project and our own assessment via an inspection of the host galaxy image. To this end, we selected a small sub-sample of images and spectra of galaxies of the highest 'spirality' (probability of being a spiral) and 'ellipticity' (probability of being an elliptical). In detail, we selected 50 nearby galaxies, five spirals, and five ellipticals of every AGN type, with redshift $z < 0.1$ in order to ensure a high-quality image. We concluded that although the Galaxy Zoo morphology classification is reliable for the majority of our galaxies, we found some cases in which the assessment of the citizens participating in the Galaxy Zoo project seems to be dubious. Our analysis showed that we can trust the characterisation of spirals up to $z \sim 0.2$ while that of ellipticals only up to $z \sim 0.1$ since the spiral features are more difficult to distinguish at higher redshifts, where a galaxy image with weak spirality can be interpreted as being an elliptical.

3. Methodology and results

This section is organised as follows. In Sect. 3.1 we study the Hubble-type frequency distributions of the host galaxies for the different samples: Sy1, Sy2, LINER, Composite, or SF, while in Sect. 3.2 we compare the projected axial-ratio (related to the orientation with respect to the line of sight) frequency distributions for the spiral hosts of Sy1s and Sy2s.

3.1. Hubble-type distribution

In this section, we seek to reveal if there is any correlation between the AGN type and the Hubble-type morphology of their host galaxies. According to the simplest unification scheme, the different AGN classes are a result of different viewing angles with respect to the orientation of an obscuring torus, and thus the properties of the host galaxies should not show any statistically significant differences. For this study, we used sub-samples of Sy1, Sy2, LINER, Composite, and SF galaxies, derived from our SDSS catalogue with a redshift limit of $z < 0.1$, in order to obtain more robust Hubble-type classification (as discussed in Sect. 2). For these sub-samples, we generated the frequency distribution of the Zoo 'ellipticity' and 'spirality' probabilities, which within the context of the simplest unification scheme, are expected to be statistically the same for all AGN classes (e.g. Antonucci 1993; Urry & Padovani 1995).

In order to be able to compare the different probability distributions, avoiding possible evolutionary effects, it is necessary to take into account any statistically significant differences between the redshift distributions of the different samples, which we present in Fig.1-(*upper panel*). Due to the different number of objects in the sub-samples, and in order to reveal systematic trends among the different sub-samples, we normalised the distributions dividing with the total number of objects in each sub-sample. Using a random sampling procedure, we matched the normalised redshift distributions to a common fractional distribution (Fig.1 - *lower panel*). Because of the low number of Sy1 galaxies and in order to avoid further depleting it, we re-sampled all other activity types, so that their normalised distributions are matched to that of the Sy1 sample.

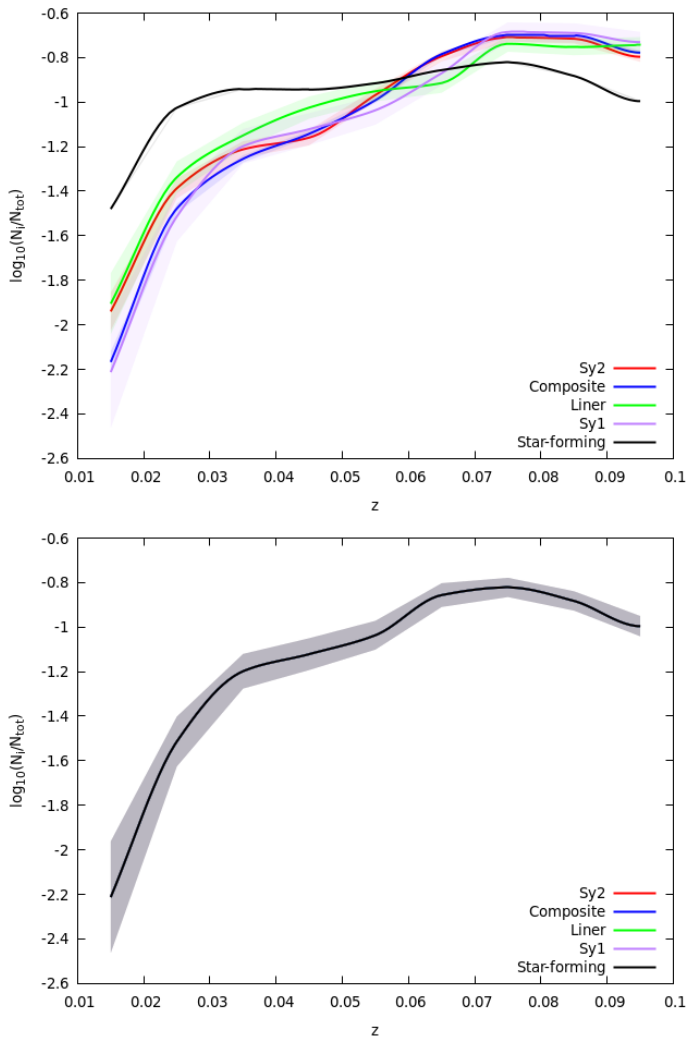


Fig. 1: *Upper panel*: Normalised redshift frequency distributions for the four sub-samples of AGN types and SF galaxies, limited to $z < 0.1$. The different sub-samples are colour-coded as denoted in the key. *Lower panel*: Redshift-matched normalised distribution. The shaded area corresponds to the 1σ Poisson uncertainty.

For the redshift-matched sub-samples, in Fig. 2 we present the ellipticity (*upper panel*) and spirality (*lower panel*) probability distributions. The two quantities are complementary, which is to be expected since the sum of the two Zoo probabilities should be roughly equal to unity. Moreover, we should note that SF galaxies, with spectra dominated by young stellar populations, are by definition spirals (Hubble 1926), and indeed, as seen in Fig. 2, their spirality distribution (black solid line) peaks at high-spirality probabilities, while their respective ellipticity distributions, which are roughly complementary, peak at zero-ellipticity probabilities. The SF galaxy sample can thus be used as a control sample of the Zoo Project spirality and ellipticity distributions of the various AGN host galaxies.

In Fig. 2, we see that the different AGN classes are distributed in the whole range of probabilities indicating a wide range of Hubble-type hosts, with the predominance of spirals. However, the normalised frequency distribution of the different AGN types are dissimilar at a statistically significant level (as indicated by the 1σ Poisson uncertainty), which implies a differ-

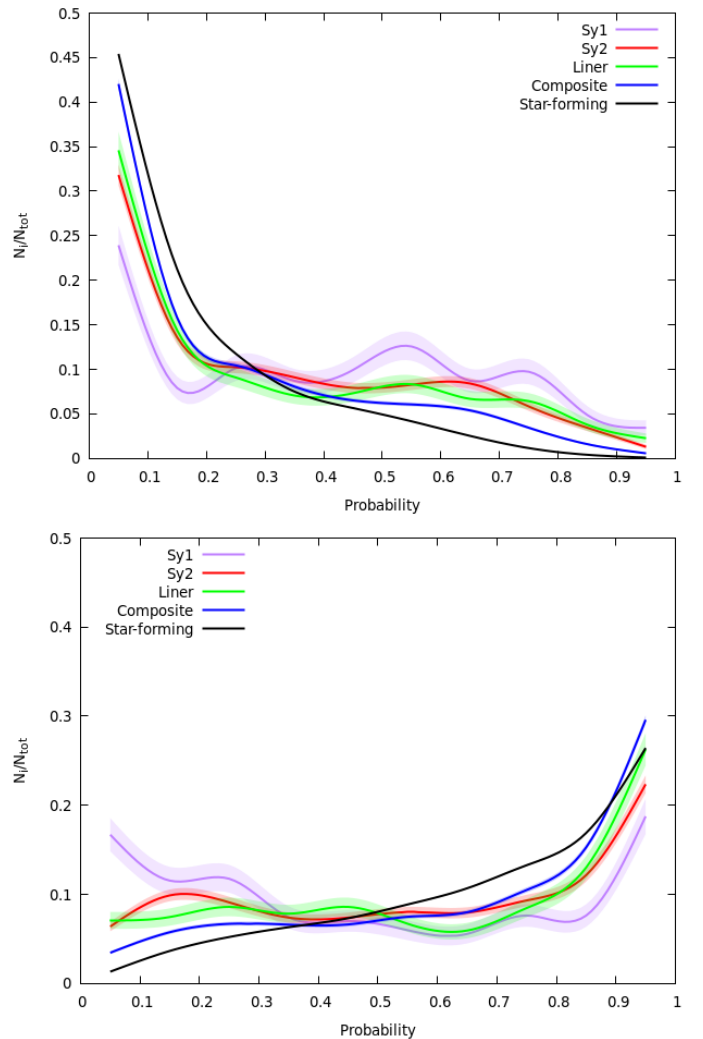


Fig. 2: Probability distributions of ellipticity (*upper panel*) and spirality (*lower panel*) for the Sy1, Sy2, LINER, Composite and SF host galaxies, limited to $z < 0.1$. The different AGN and SF sub-samples are colour-coded as in Fig. 1, while the shaded area corresponds to the 1σ Poisson uncertainty.

ent Hubble-type distribution for the different AGN types, a result that contradicts the original unification paradigm according to which there should be no dependence of the AGN class on the host galaxy's Hubble-type classification (e.g. Antonucci 1993). Interestingly, the Sy1s show a peak at both high- and low- spirality probabilities, indicating a relatively higher fraction of Sy1s, with respect to other AGN types, residing in elliptical hosts.

For a more revealing comparison of the previously discussed morphology difference of the various AGN host galaxies with respect to SF galaxies, in Fig. 3 we present the excess factor by which the fractional number of the various AGN types exceeds that corresponding to SF galaxies, for each spirality or ellipticity probability:

$$\Delta(\text{AGN}, p) = \frac{N_i(\text{AGN})/N_{\text{tot}}(\text{AGN})}{N_i(\text{SF})/N_{\text{tot}}(\text{SF})} - 1.$$

Upon inspecting Fig. 3, it becomes evident that Sy1s show the highest relative preference for elliptical hosts with respect to LINERs, Sy2s, and Composites, although all AGN types, each at a different degree, appear in elliptical hosts.

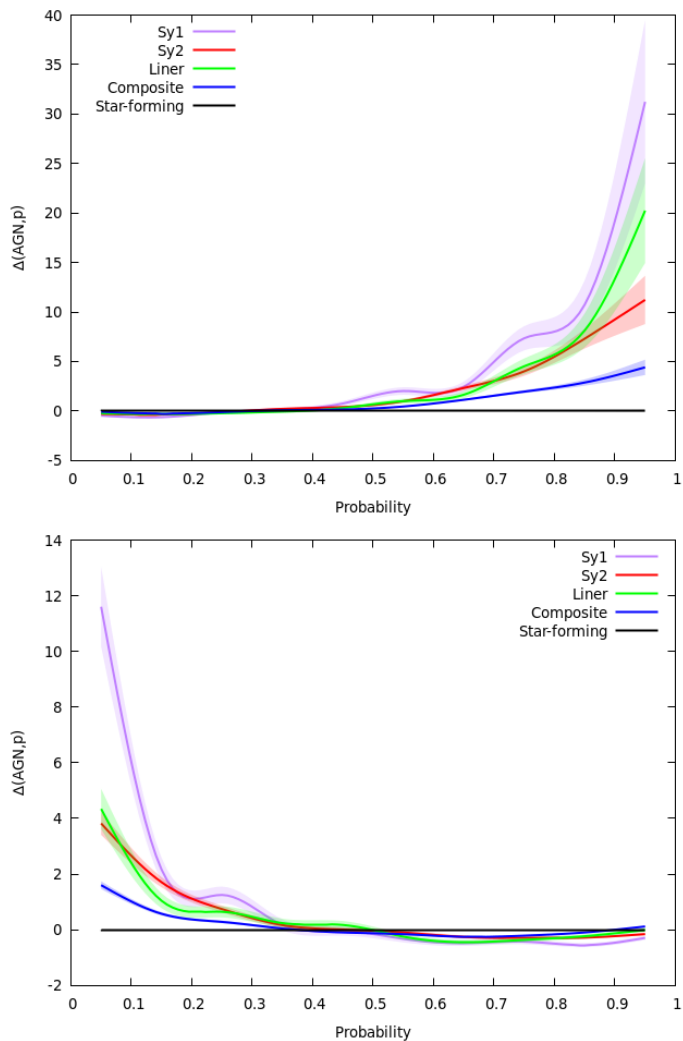


Fig. 3: Values of the factor $\Delta(\text{AGN}, p)$ by which the different AGN types exceed the corresponding fractional number of SF galaxies for the ellipticity (*upper panel*) and spirality (*lower panel*) cases. The different AGN and SF sub-samples are colour-coded as in Fig.1, while the shaded area corresponds to the 1σ Poisson uncertainty.

3.2. Effect of the galactic disc on the obscuration of the AGN

We wish to test the hypothesis that the AGN host galaxy contributes to the obscuration of the AGN emission. To this end, we studied the orientation of spiral galaxies hosting Sy1 and Sy2 nuclei, limited to $z < 0.2$. We only selected spiral hosts for this test since the orientation of spirals with respect to the line of sight can be quantified via their projected axis ratio, (b/a) . Furthermore, in order to reduce noise, we required a high Galaxy Zoo spirality probability, that is $p > 0.8$. We also used the corresponding sub-sample of SF galaxies as a reference (or control) sample.

3.2.1. Matching the redshift distributions

In Figs.4-5-(*upper panel*), we present the Sy1 and Sy2 sub-sample normalised redshift distributions and compare them with the corresponding distribution of SF galaxies. As can be clearly seen, and also as quantified by the Kolmogorov-Smirnov (KS) test (p -value ~ 0 and $\sim 10^{-4}$, respectively), the distributions are

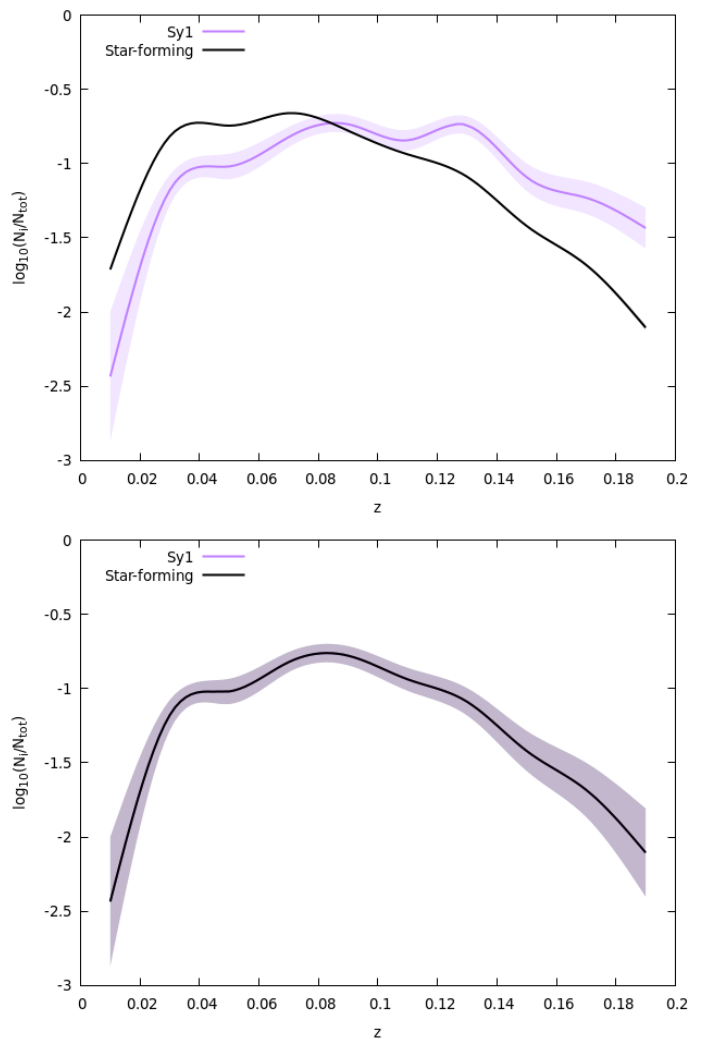


Fig. 4: *Upper panel*: Normalised redshift distribution of spiral Sy1 and SF galaxies. *Lower panel*: Normalised redshift-matched distribution of Sy1s and the corresponding SF control sample. The Sy1 and the SF sub-samples are colour-coded as in Fig.1, while the shaded area corresponds to the 1σ Poisson uncertainty.

significantly different. For $z \lesssim 0.08$, the fraction of both the AGN populations is lower than that of the SF galaxies, while for higher values, $z \gtrsim 0.1$, the AGN fractions are greater than that of SF galaxies. Whether due to observational biases or evolutionary effects, understanding such differences is out of the scope of the current work. However, we needed to ensure that our results would not be affected by such biases and thus followed the same re-sampling technique as in Sect. 3.1, in order to obtain matched-redshift distributions, which are shown in Figs. 4-5 - (*lower panel*).

We can now proceed to a meaningful comparison of the orientation distribution of Sy1s and Sy2s with respect to the SF case. We expect that, according to the simplest unification model, the orientation distributions of Sy1s and Sy2s hosted in spiral galaxies must be identical to that of spiral SF galaxies. In presenting our results, we again normalise the distributions by the total number of objects in each sub-sample.

In Fig.6, we present the comparative plot of the normalised axis-ratio (b/a) distributions for the spiral galaxies hosting Sy1 nuclei (purple) and for the control sample of SF galaxies. It is

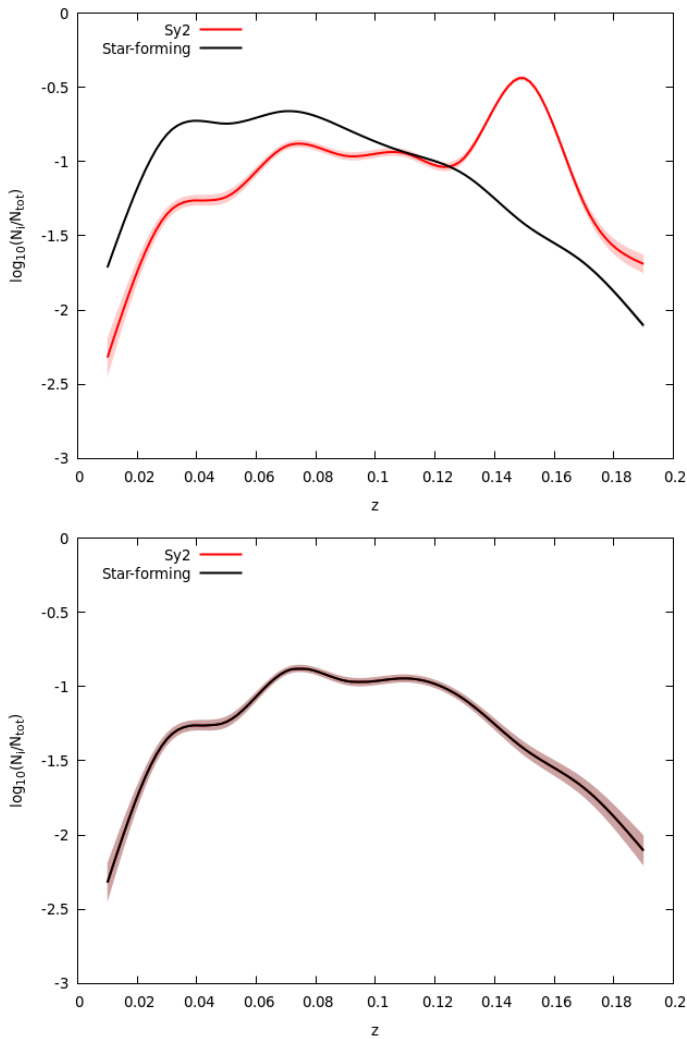


Fig. 5: *Upper panel*: Normalised redshift distribution of spiral Sy2 and SF galaxies. *Lower panel*: Normalised redshift-matched distribution of Sy2 and the corresponding SF control sample. The Sy2 and the SF sub-samples are colour-coded as in Fig.1, while the shaded area corresponds to the 1σ Poisson uncertainty.

evident that the two distributions are different, which we also confirm with a KS test (p -value $\sim 10^{-8}$); the b/a distribution of Sy1 is skewed towards high b/a values, indicating inclination angles closer to face-on orientations, while the control sample covers the full range of orientation angles. The distribution of the control sample shows a peak at $b/a \approx 0.35$, whereas the Sy1 population peaks at $b/a \approx 0.7$. Moreover, for $b/a < 0.4$ we find that the fraction of Sy1 host galaxies decreases dramatically compared to SF galaxies. Thus, we conclude that the type 1 Seyferts tend to be more 'face-on' compared to SF galaxies, and only a very small fraction of Sy1 galaxies are found to have b/a values close to the edge-on orientation.

In Fig. 7, we present the respective b/a comparison plot for the Sy2 and the star-forming subsamples, and we find that although their distributions are significantly more similar than the corresponding of Fig.6, they are still statistically different as confirmed by a KS test (p -value $\sim 10^{-11}$). In detail, both the type 2 Seyferts and the SF galaxies are distributed in the whole range of b/a , with the star-forming peaking at $b/a \approx 0.35$, while the Sy2 appear to have two local maxima, at $b/a \approx 0.37$ and at $b/a \approx 0.65$.

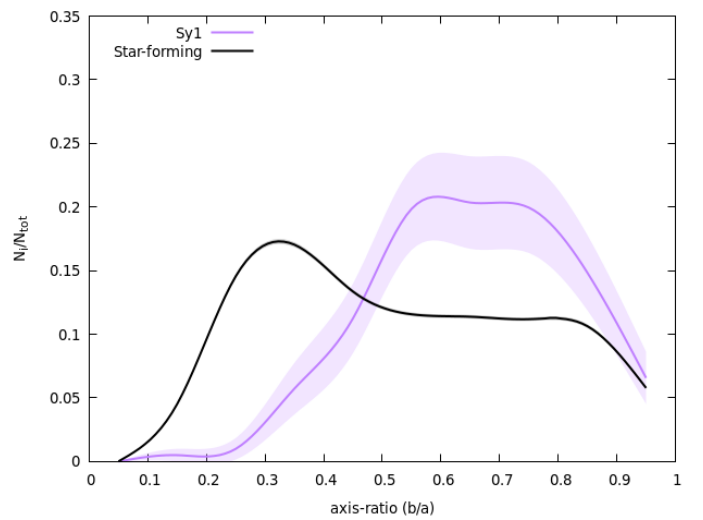


Fig. 6: Distribution of the projected axial ratio for spiral galaxies hosting Sy1s and the corresponding control sample of SF galaxies. The Sy1 and the SF sub-samples are colour-coded as in Fig.1, while the shaded area corresponds to the 1σ Poisson uncertainty.

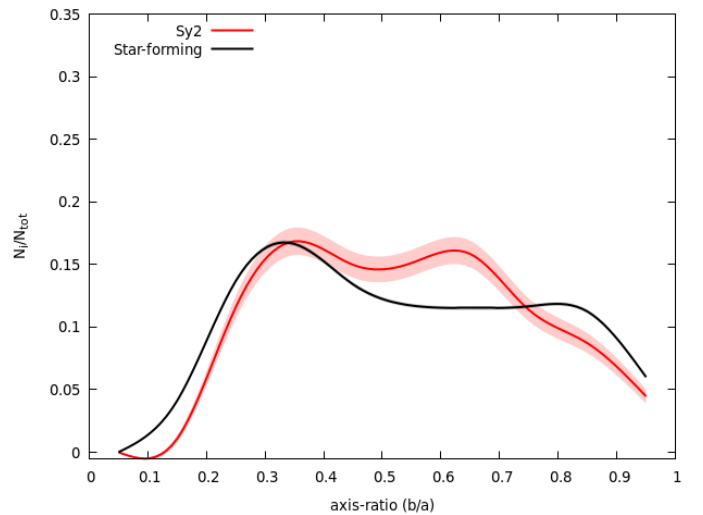


Fig. 7: Distribution of projected axial ratios for spiral galaxies hosting type 2 AGNs and the corresponding control SF sample. The Sy2 and the SF sub-samples are colour-coded as in Fig.1, while the shaded area corresponds to the 1σ Poisson uncertainty.

A significantly higher fraction of Sy2 galaxies has values of $b/a \in (0.3, 0.8)$, while for values $b/a < 0.3$ (close to edge-on orientations) and $b/a > 0.8$ (close to face-on orientations), the fraction of Sy2s is lower than that of SF galaxies.

3.2.2. Matching stellar mass distributions

Comparing AGN samples of different intrinsic luminosity distributions may introduce a bias to the results. To this end, one could use physical properties that are proxies of the AGN intrinsic luminosity, as the luminosity of [O III]5007 emission line or the stellar mass of the host galaxies. However, since we are

studying the additional absorption by the host galaxy that may also obscure the NLR, the use of the [OIII] line can bias our results. Therefore, we chose to match the stellar mass distributions of our samples, derived by the MPA-JHU teams, using the methodology defined in Kauffmann et al. (2003) and applied to photometric data as described in Salim et al. (2007). Furthermore, this normalisation eliminates any possible bias introduced by the excessive absorption in one of the samples because of the uneven distribution of massive hosts.

For the already redshift-matched samples, in Fig.8 we present the normalised stellar mass distributions of type 1 (*upper panel*) and type 2 (*lower panel*) AGNs with the corresponding distribution of SF galaxies. It is evident, but also confirmed by a KS test, that the distributions are statistically different (p -value ~ 0). We find that both AGN classes are identified with more massive host galaxies compared to the sample of SF galaxies, a result which is in agreement with that of Bornancini & García Lambas (2020). Even though the direct comparison of the Sy1 and Sy2 stellar mass distributions is out of the scope of this work, it is noteworthy to mention that many previous studies (e.g. Yang et al. 2017; Yang et al. 2019) have shown that both AGN types have similar stellar mass hosts (see discussion in Zou et al. (2019)), which we also confirmed by a simple inspection of the corresponding figures.

In order to acquire more robust results and to ensure the removal of possible luminosity biases we follow the same re-sampling technique, as in Sect. 3.1, to obtain matched stellar-mass distributions, which are shown in Fig. 8 (dashed distributions), at the expense, however, of significantly reducing the size of the AGN samples. This also excludes the most massive host galaxies from our samples, which could indeed reduce the significance of the effect (galaxy-disc obscuration of nuclear region) that we are seeking to investigate.

We can now detail the axial-ratio (b/a) distributions for the spiral-redshift- and stellar-mass-matched sub-samples of Sy1, Sy2, and star-forming galaxies. In Fig.9, we present the normalised b/a comparative plot for Sy1 galaxies and the corresponding control sample. The KS test confirmed that the two distributions are different (p -value $\sim 10^{-3}$). Compared to Fig.6, despite the reduction of the Sy1 sample size, both plots show similar behaviours, confirming that the results obtained in Sect. 3.2.1 are robust.

Correspondingly, in Fig.10 we present the normalised comparative plot for Sy2 and SF galaxies, and again the resulting distributions are similar to those of Fig.7, again confirming that the main results presented in Sect. 3.2.1 are robust. However, in this case there is a small but distinct difference at small b/a values with the fraction of Sy2 being lower than that of SF for $b/a < 0.2$, in contrast with Fig.7 where this transition occurs for $b/a \approx 0.3$. Thus, when matching to stellar mass (Fig.10), the fraction of Sy2 with small b/a is not significantly different to that of SF galaxies (Fig.7).

4. Discussion

4.1. Why do Sy1 nuclei favour elliptical hosts?

There are various indications for differences in the host galaxies of AGNs in the literature. Our results in the low-redshift regime are in agreement with the results of Bornancini & García Lambas (2018), based on higher redshift ($0.3 < z < 1.1$) type 1 and type 2 AGNs from the COSMOS2015 catalogue, who showed that the type 1 AGN host galaxies appear more elliptical and compact than those of type 2 AGNs that span the whole spiral

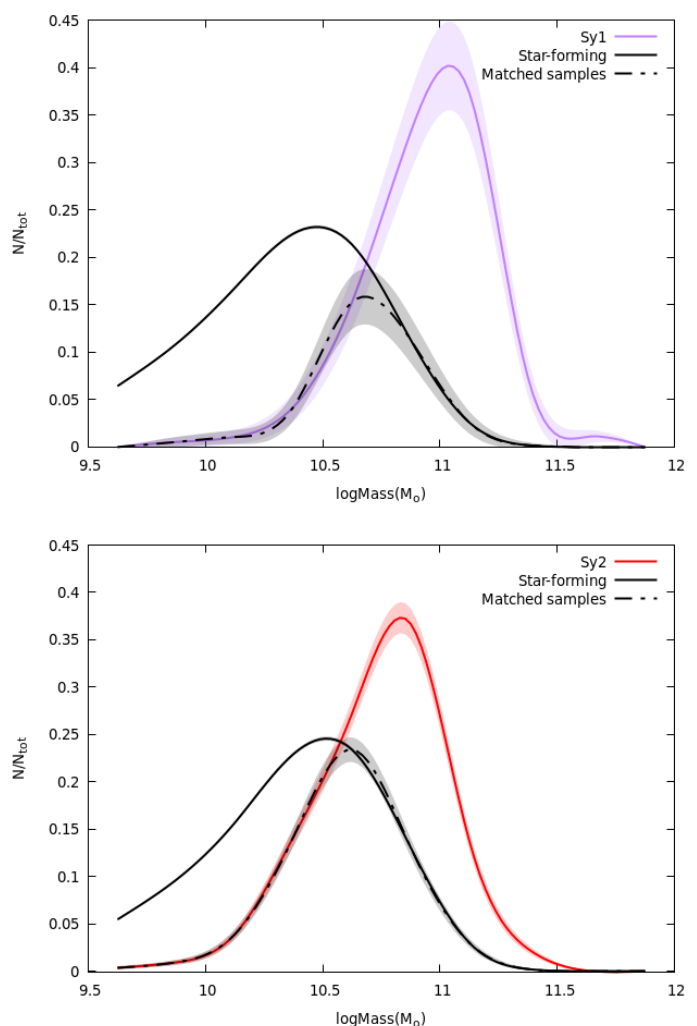


Fig. 8: Normalised stellar-mass distribution of spiral Sy1 (*upper panel*) and Sy2 (*lower panel*) with the corresponding SF and stellar-mass-matched sample (dashed line). The Sy1, Sy2, and SF sub-samples are colour-coded as in Fig.1, while the shaded area corresponds to the 1σ Poisson uncertainty.

to elliptical Hubble-type range. In addition, using data from the fourth SDSS Data Release (DR4), Sorrentino et al. (2006) found that 76% of type 1 Seyfert host galaxies are elliptical, while the corresponding ratio of Seyfert 2 hosted in early-type galaxies is 56.8%. Slavcheva-Mihova & Mihov (2011) found that more type 1 than type 2 AGNs prefer elliptical hosts. Similarly, Villarroel et al. (2017) and Chen & Hwang (2017) concluded that Sy2 nuclei reside more in spiral hosts ($\sim 30 - 40\%$) than Sy1 nuclei do ($\sim 20\%$), in disagreement with the simplest unification model.

The different bulge distributions of Sy1 and Sy2 might be related to an evolutionary sequence of AGN activity (e.g. Krongold et al. 2002; Tran 2003; Koulouridis et al. 2006; Villarroel et al. 2012; Koulouridis et al. 2013; Villarroel & Korn 2014). These results indicate a possible co-evolution scheme between galaxies and SMBHs (e.g. Springel et al. 2005; Hopkins et al. 2006, 2008b,a; Madau & Dickinson 2014) (see also reviews by Kormendy & Ho 2013; Heckman & Best 2014).

At the initial merging phase, during the enhanced star-forming activity and accretion, the AGN is mostly obscured because of the large amount of gas and dust in the circum-nuclear

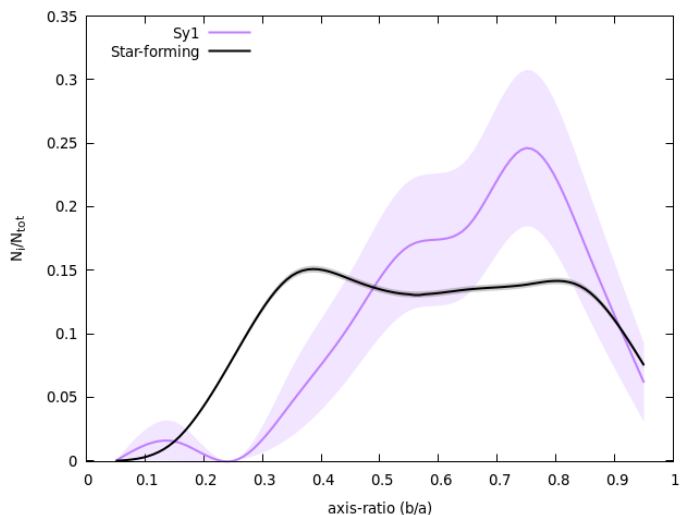


Fig. 9: Distribution of the projected axial ratio for stellar-mass-matched spiral galaxies hosting Sy1s and the corresponding control sample of SF galaxies. The Sy1 and SF sub-samples are colour-coded as in Fig.1, while the shaded area corresponds to the 1σ Poisson uncertainty.

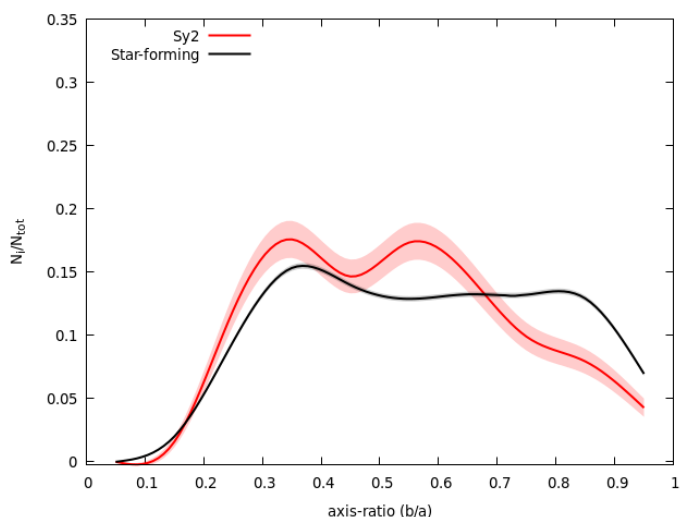


Fig. 10: Distribution of the projected axial ratio for stellar-mass-matched spiral galaxies hosting Sy2s and the corresponding control sample of SF galaxies. The Sy2 and SF sub-samples are colour-coded as in Fig.1, while the shaded area corresponds to the 1σ Poisson uncertainty.

region. However, the AGN will eventually be revealed after the surrounding material is consumed, or expelled by radiation pressure. In parallel to the AGN evolution, the stellar population of the merger will also rapidly redden and the host will eventually be transformed to a quiescent elliptical galaxy (e.g. Hopkins et al. 2008b,a). AGN feedback plays an essential role in both AGN and galaxy transformation and probably leads to the observed SMBH-bulge relation (e.g. Magorrian et al. 1998; Ferrarese & Merritt 2000; Gebhardt et al. 2000). Although, major mergers and powerful AGNs are far less common in the local Universe, compared to redshift $z > 1$, the difference found in the

current work could be partly due to the co-evolution of the bulge and AGN activity after such events.

Alternatively, or in addition, the difference could also be due to the obscuration of the BLR from the gas- and dust-rich disc of a spiral galaxy, especially in edge-on systems. This possibility is discussed further in the next section.

4.2. Why do Sy1 nuclei favour face-on orientations of the host galaxy?

Our analysis also showed that the orientations of the Sy1 and Sy2 spiral host galaxies are significantly different when compared to the control sample of the spiral SF galaxies. This is also unexpected within the simplest unification scheme, and the interpretation of our results points towards two possible scenarios:

1. additional obscuration of the AGN by dust in the galactic disc near the circum-nuclear region
2. some level of statistical co-alignment of the plane of the torus and that of the galactic disc.

According to the latter scenario, Sy1 galaxies, which have a 'face-on' torus, also have more frequently face-on host galaxy orientations. However, if that is the case, we should correspondingly expect a higher fraction of 'edge-on' host galaxies in the Sy2 distribution with respect to SF galaxies, but this is not observed. Without excluding this scenario, since processes like merging may induce a rearrangement and facilitate such a coplanarity, we do not have a clear indication to confirm this hypothesis (see, however, Maiolino & Rieke (1995) for a relevant discussion).

Our results favour the scenario where additional obscuration, caused by the host galaxy, might affect the classification of Seyfert types, regardless of the inclination of the torus, as also claimed by Lagos et al. (2011). This result is similar to the one found by Keel (1980), who was the first to discover a deficiency of Sy1 galaxies in edge-on hosts (see also Lawrence & Elvis 1982). Recent works support the idea that galactic-scale dust is responsible for additional obscuration (e.g. Burtscher et al. 2016). Buchner & Bauer (2017) showed that a large fraction (up to 40%) of the obscuration observed in AGNs, at least in the Compton-thin regime, is not due to the nuclear torus, but to the galaxy-scale gas in the host, while DiPompeo et al. (2017b) estimated the fraction of IR-selected type 2 AGNs that are obscured by dust outside the torus to be $\sim 25\%$. Also, using data from the intermediate Palomar Transient Factory, the SDSS DR7, and Galaxy Zoo, Villarroel et al. (2017) found that for the majority of Sy2 galaxies (up to 90%), the obscuration must stem from larger scales: host galaxy obscuration and/or a large-scale environment in which the host galaxies reside.

Furthermore, having studied a sample of nearby Compton-thick AGNs, Goulding et al. (2012) concluded that the dust of the host galaxy, and not necessarily the compact torus, is the dominant obscurer of the central engine. Using Spitzer data of six $0.3 < z < 0.8$ type 2 quasars, Lacy et al. (2007) found a contribution of the extinction towards the nucleus from an extended star-forming disc on scales of kiloparsecs, in addition to, or instead of, the traditional dusty torus. Moreover, also using high-redshift type 2 quasars from Spitzer and VLA data of the Spitzer First Look Survey, Martínez-Sansigre et al. (2006b) concluded that the nuclear region could be effectively obscured by dust on large scales, away from the torus. Additionally, using X-ray-selected AGNs with spectroscopic redshifts in the Chandra Deep Field South (CDFs), Rigby et al. (2006) argued that part of the column density that obscures the soft X-rays may come

from the galactic disc. Last but not least, Malizia et al. (2020) used the hard X-ray-selected sample of AGNs detected by INTEGRAL/IBIS to show that material located in the host galaxy on scales of hundreds of parsecs and not aligned with the absorbing torus can sufficiently hide the BLR of some type 1 AGNs, causing their classification as type 2 objects and giving rise to the deficiency of type 1 in edge-on galaxies.

Although the deficiency of edge-on Sy1 galaxies is unexpected in the simplest unification model, it does not necessarily contradict it. It might be assumed that in the case of edge-on Seyfert galaxies the gas and dust along the host galaxy disc can act in the same way as the torus, blocking the direct view of the BLR, thus leading to a classification as a Sy2 galaxy (e.g. Schmitt et al. 2001).

4.3. Why there is a deficit of Sy2 nuclei in edge-on and face-on spiral hosts with respect to SF galaxies?

Regarding the small but significant difference in the b/a distributions of the spiral Sy2 and SF galaxies (Fig.7), at low b/a values a possible explanation could be that in extreme edge-on orientations the dust of the galactic disc can obscure not only the BLR but also the NLR region. In an early study, McLeod & Rieke (1995) used samples of optically and soft-X-ray-selected Seyferts and found a bias against inclined spiral hosts, while hard-X-ray-selected samples were found unbiased. In addition, Malkan et al. (1998) argued that in Sy2 galaxies irregular structures at large distances can provide sufficient absorbing column density for the nuclear source. Similar results were presented in Rigby et al. (2006), where they attributed the appearance of X-ray-selected AGNs as optically 'dull' to galactic absorption.

On the other hand, there is a hypothesis that low luminosity Seyferts may be diluted by high-luminosity host galaxies, in which the continuum can hide the AGN lines. This may be the case for high- z AGNs, where the source fully falls within the spectroscopic fiber or slit, as demonstrated by Moran & Filippenko (2002) and later supported by Trump et al. (2009) for a sample of high- z dull AGNs in the COSMOS survey. However, our sample is limited to $z < 0.2$, and furthermore, relevant studies showed that there is no significant dilution in dull local AGN samples (La Franca et al. 2002; Hornschemeier et al. 2005). In addition, Rigby et al. (2006) argued against dilution also in high- z AGNs. Therefore, we do not consider this scenario as a possible explanation for our results. A co-alignment of the torus with the disc cannot explain the deficit of Sy2 galaxies in edge-on systems either when compared with the control SF sample.

Finally, we note that the smaller (higher) fraction of Sy2 (Sy1) with respect to SF galaxies at high b/a values strengthens the hypothesis of a host galaxy contribution to the obscuration of the BLR. Specifically, due to the fact that in face-on galaxies the gas and the dust of the disc does not intervene between the observer and the active nuclei, the only obscurer of the BLR is the torus, which apparently in some cases is not sufficient to hide the BLR, giving rise to the deficiency of type 2 in face-on galaxies (e.g. Lacy et al. 2007).

In the context of matching the samples of Sy1, Sy2, and control SF galaxies to stellar mass, the lack of 'hidden' Sy2 at small b/a values compared to the unmatched case can be explained, as we point out in Sect. 3.2.2, by the fact that the matching procedure cuts the most massive Sy2 and Sy1 galaxies, which are also the most abundant. Taking into account that more massive spiral galaxies contain more dust (e.g. Whitaker et al. 2017), by excluding them from our samples we effectively exclude those host galaxies that can obscure both the AGN BLR and the NLR

at extreme edge-on configurations. This result further supports the scenario of a host galaxy contribution to the obscuration of the AGN activity.

5. Conclusions

The main purpose of the current work was to test aspects of the simplest unification paradigm by searching for differences in the properties of the host galaxies of various AGN types. For our purposes, we used (a) the SDSS DR14 spectroscopic galaxy catalogue, selecting sub-samples of Sy1 and Sy2, LINER, Composite and SF galaxies, limited to $z < 0.2$, and (b) the results of the Galaxy Zoo project regarding the Hubble-type morphology of these galaxies.

Our main results are listed below:

1. We find statistically significant differences -quantified by a KS two-sample test- of the various types of AGN host-galaxy Hubble types, with the most significant result being that the fraction of Sy1 galaxies hosted by ellipticals is higher than that of any other AGN class. These results can be interpreted within a possible co-evolution scenario between galaxies and SMBs.
2. We also find that the orientation distributions, as revealed by the disc axis ratio (b/a) of the Sy1 and Sy2 spiral populations show statistically significant differences with respect to the control sample of star-forming galaxies (which by definition should cover all possible orientation configurations), which is in conflict with the predictions of the simple unified model. These differences hint towards an effect by which the dusty galactic disc has a significant contribution to the obscuration of the broad-line and partially also of the narrow-line nuclear region. This could also interpret our previous result regarding the host-galaxy Hubble types of type 1 AGN. Indeed, the fact that we detect more Sy1 than any other AGN type in elliptical hosts (which as is well known are gas and dust deficient) can be explained if the amount of galactic dust and gas contributes to the obscuration of the nuclear region and in particular the BLR.

These findings are at odds with the expectations of the simplest formulation of the unification paradigm, implying that beyond the orientation of the torus, at least two other factors play an important role in the AGN classification: (a) the orientation of the host galaxy, and (b) evolution.

Acknowledgements. Authors thank the anonymous referee for useful comments which helped us improve the presentation of this work. This paper has made use of the data from the SDSS projects. Funding for the Sloan Digital Sky Survey IV has been provided by the Alfred P. Sloan Foundation, the U.S. Department of Energy Office of Science, and the Participating Institutions. SDSS-IV acknowledges support and resources from the Center for High-Performance Computing at the University of Utah. The SDSS web site is www.sdss.org. SDSS-IV is managed by the Astrophysical Research Consortium for the Participating Institutions of the SDSS Collaboration including the Brazilian Participation QUASAR BLACK HOLE MASSES 25 Group, the Carnegie Institution for Science, Carnegie Mellon University, the Chilean Participation Group, the French Participation Group, Harvard-Smithsonian Center for Astrophysics, Instituto de Astrofísica de Canarias, The Johns Hopkins University, Kavli Institute for the Physics and Mathematics of the Universe (IPMU) / University of Tokyo, the Korean Participation Group, Lawrence Berkeley National Laboratory, Leibniz Institut für Astrophysik Potsdam (AIP), Max-Planck-Institut für Astronomie (MPIA Heidelberg), Max-Planck-Institut für Astrophysik (MPA Garching), Max-Planck-Institut für Extraterrestrische Physik (MPE), National Astronomical Observatories of China, New Mexico State University, New York University, University of Notre Dame, Observatorio Nacional / MCTI, The Ohio State University, Pennsylvania State University, Shanghai Astronomical Observatory, United Kingdom Participation Group, Universidad Nacional Autónoma de México, University of Arizona, University of Colorado Boulder, University

of Oxford, University of Portsmouth, University of Utah, University of Virginia, University of Washington, University of Wisconsin, Vanderbilt University, and Yale University.

References

- Abolfathi, B., Aguado, D. S., Aguilar, G., et al. 2018, *ApJS*, 235, 42
- Antonucci, R. 1993, *ARA&A*, 31, 473
- Audibert, A., Riffel, R., Sales, D. A., Pastoriza, M. G., & Ruschel-Dutra, D. 2017, *MNRAS*, 464, 2139
- Baldwin, J. A., Phillips, M. M., & Terlevich, R. 1981, *PASP*, 93, 5
- Bitsakis, T., Charmandaris, V., Le Floch, E., et al. 2010, *A&A*, 517, A75
- Bornancini, C. & García Lambas, D. 2018, *MNRAS*, 479, 2308
- Bornancini, C. & García Lambas, D. 2020, *MNRAS*, 494, 1189
- Bornancini, C. G., Taormina, M. S., & Lambas, D. G. 2017, *A&A*, 605, A10
- Brinchmann, J., Charlot, S., Heckman, T. M., et al. 2004, arXiv e-prints, astro
- Buchner, J. & Bauer, F. E. 2017, *MNRAS*, 465, 4348
- Burtscher, L., Davies, R. L., Graciá-Carpio, J., et al. 2016, *A&A*, 586, A28
- Chen, C.-T. J., Hickox, R. C., Alberts, S., et al. 2015, *ApJ*, 802, 50
- Chen, Y.-C. & Hwang, C.-Y. 2017, *Astrophysics and Space Science*, 362
- DiPompeo, M. A., Hickox, R. C., Eftekharzadeh, S., & Myers, A. D. 2017a, *MNRAS*, 469, 4630
- DiPompeo, M. A., Hickox, R. C., Myers, A. D., & Geach, J. E. 2017b, *MNRAS*, 464, 3526
- Elitzur, M. 2012, *ApJ*, 747, L33
- Elitzur, M. & Ho, L. C. 2009, *ApJ*, 701, L91
- Elitzur, M., Ho, L. C., & Trump, J. R. 2014, *MNRAS*, 438, 3340
- Elitzur, M. & Shlosman, I. 2006, *ApJ*, 648, L101
- Ferrarese, L. & Merritt, D. 2000, *ApJ*, 539, L9
- Gebhardt, K., Bender, R., Bower, G., et al. 2000, *ApJ*, 539, L13
- González, J. J., Krongold, Y., Dultzin, D., et al. 2008, in *Revista Mexicana de Astronomía y Astrofísica Conference Series*, Vol. 32, *Revista Mexicana de Astronomía y Astrofísica Conference Series*, 170–172
- Goulding, A. D., Alexander, D. M., Bauer, F. E., et al. 2012, *ApJ*, 755, 5
- He, Z., Sun, A.-L., Zakamska, N. L., et al. 2018, *MNRAS*, 478, 3614
- Heckman, T. M. & Best, P. N. 2014, *ARA&A*, 52, 589
- Hernández-Ibarra, F. J., Krongold, Y., Dultzin, D., et al. 2016, *MNRAS*, 459, 291
- Hickox, R. C. & Alexander, D. M. 2018, *ARA&A*, 56, 625
- Hopkins, P. F., Cox, T. J., Kereš, D., & Hernquist, L. 2008a, *ApJS*, 175, 390
- Hopkins, P. F., Hernquist, L., Cox, T. J., et al. 2006, *ApJS*, 163, 1
- Hopkins, P. F., Hernquist, L., Cox, T. J., & Kereš, D. 2008b, *ApJS*, 175, 356
- Hornschemeier, A. E., Heckman, T. M., Ptak, A. F., Tremonti, C. A., & Colbert, E. J. M. 2005, *AJ*, 129, 86
- Hubble, E. 1926, *Contributions from the Mount Wilson Observatory / Carnegie Institution of Washington*, 324, 1
- Jiang, N., Wang, H., Mo, H., et al. 2016, *ApJ*, 832, 111
- Kauffmann, G., Heckman, T. M., White, S. D. M., et al. 2003, *MNRAS*, 341, 54
- Keel, W. C. 1980, *AJ*, 85, 198
- Kinney, A. L., Schmitt, H. R., Clarke, C. J., et al. 2000, *The Astrophysical Journal*, 537, 152–177
- Kormendy, J. & Ho, L. C. 2013, *ARA&A*, 51, 511
- Koulouridis, E. 2014, *A&A*, 570, A72
- Koulouridis, E., Plionis, M., Chavushyan, V., et al. 2013, *A&A*, 552, A135
- Koulouridis, E., Plionis, M., Chavushyan, V., et al. 2006, *ApJ*, 639, 37
- Krongold, Y., Dultzin-Hacyan, D., & Marziani, P. 2002, *ApJ*, 572, 169
- La Franca, F., Fiore, F., Vignali, C., et al. 2002, *ApJ*, 570, 100
- Lacy, M., Sajina, A., Petric, A. O., et al. 2007, *ApJ*, 669, L61
- Lagos, C. D. P., Padilla, N. D., Strauss, M. A., Cora, S. A., & Hao, L. 2011, *MNRAS*, 414, 2148
- Lanzuisi, G., Delvecchio, I., Berta, S., et al. 2017, *A&A*, 602, A123
- Lawrence, A. & Elvis, M. 1982, *ApJ*, 256, 410
- Lintott, C. J., Schawinski, K., Slosar, A., et al. 2008, *MNRAS*, 389, 1179
- Madau, P. & Dickinson, M. 2014, *Annual Review of Astronomy and Astrophysics*, 52, 415–486
- Magorrian, J., Tremaine, S., Richstone, D., et al. 1998, *AJ*, 115, 2285
- Maiolino, R. & Rieke, G. H. 1995, *ApJ*, 454, 95
- Malizia, A., Bassani, L., Stephen, J. B., Bazzano, A., & Ubertaini, P. 2020, *A&A*, 639, A5
- Malkan, M. A., Gorjian, V., & Tam, R. 1998, *ApJS*, 117, 25
- Martínez, M. A., del Olmo, A., Coziol, R., & Focardi, P. 2008, *ApJ*, 678, L9
- Martínez-Sansigre, A., Rawlings, S., Lacy, M., et al. 2006a, *Astronomische Nachrichten*, 327, 266
- Martínez-Sansigre, A., Rawlings, S., Lacy, M., et al. 2006b, *Astronomische Nachrichten*, 327, 266
- Masoura, V. A., Mountrichas, G., Georgantopoulos, I., & Plionis, M. 2021, arXiv e-prints, arXiv:2101.00724
- Matt, G. 2000, *A&A*, 355, L31
- McLeod, K. K. & Rieke, G. H. 1995, *ApJ*, 441, 96
- Melnyk, O., Elyiv, A., Smolčić, V., et al. 2018, *A&A*, 620, A6
- Mendoza-Castrejón, S., Dultzin, D., Krongold, Y., González, J. J., & Elitzur, M. 2015, *MNRAS*, 447, 2437
- Moran, E. C. & Filippenko, A. V. 2002, in *American Astronomical Society Meeting Abstracts*, Vol. 200, *American Astronomical Society Meeting Abstracts #200*, 17.04
- Netzer, H. 2015, *ARA&A*, 53, 365
- Nicastro, F., Martocchia, A., & Matt, G. 2003, *ApJ*, 589, L13
- Perlman, E. S., Mason, R. E., Packham, C., et al. 2007, *ApJ*, 663, 808
- Powell, M. C., Cappelluti, N., Urry, C. M., et al. 2018, *The Astrophysical Journal*, 858, 110
- Prieto, M. A., Mezcuca, M., Fernández-Ontiveros, J. A., & Schartmann, M. 2014, *MNRAS*, 442, 2145
- Raddick, J., Lintott, C. J., Schawinski, K., et al. 2007, in *American Astronomical Society Meeting Abstracts*, Vol. 211, 94.03
- Ramos Almeida, C., Levenson, N. A., Alonso-Herrero, A., et al. 2011, *The Astrophysical Journal*, 731, 92
- Rigby, J. R., Rieke, G. H., Donley, J. L., Alonso-Herrero, A., & Pérez-González, P. G. 2006, *ApJ*, 645, 115
- Salim, S., Rich, R. M., Charlot, S., et al. 2007, *ApJS*, 173, 267
- Schmitt, H. R., Antonucci, R. R. J., Ulvestad, J. S., et al. 2001, *ApJ*, 555, 663
- Siebenmorgen, R., Heymann, F., & Efstathiou, A. 2015, *A&A*, 583, A120
- Slavcheva-Mihova, L. & Mihov, B. 2011, *A&A*, 526, A43
- Sorrentino, G., Radovich, M., & Rifatto, A. 2006, *A&A*, 451, 809
- Spinoglio, L. & Fernández-Ontiveros, J. A. 2019, arXiv e-prints, arXiv:1911.12176
- Springel, V., Di Matteo, T., & Hernquist, L. 2005, *MNRAS*, 361, 776
- Suh, H., Civano, F., Hasinger, G., et al. 2019, *The Astrophysical Journal*, 872, 168
- Tran, H. D. 2001, *ApJ*, 554, L19
- Tran, H. D. 2003, *ApJ*, 583, 632
- Tremonti, C. A., Heckman, T. M., Kauffmann, G., et al. 2004, *ApJ*, 613, 898
- Trump, J. R., Impey, C. D., & Kelly, B. C. 2011, in *American Astronomical Society Meeting Abstracts*, Vol. 217, *American Astronomical Society Meeting Abstracts #217*, 430.08
- Trump, J. R., Impey, C. D., Taniguchi, Y., et al. 2009, *ApJ*, 706, 797
- Urry, C. M. & Padovani, P. 1995, *PASP*, 107, 803
- Villarroel, B., Korn, A., & Matsuoka, Y. 2012, arXiv e-prints, arXiv:1211.0528
- Villarroel, B. & Korn, A. J. 2014, *Nature Physics*, 10, 417
- Villarroel, B., Nyholm, A., Karlsson, T., et al. 2017, *ApJ*, 837, 110
- Whitaker, K. E., Pope, A., Cybulski, R., et al. 2017, *ApJ*, 850, 208
- Yang, G., Brandt, W. N., Alexander, D. M., et al. 2019, *MNRAS*, 485, 3721
- Yang, G. et al. 2017, *Astrophys. J.*, 842, 72
- Zou, F., Yang, G., Brandt, W. N., & Xue, Y. 2019, arXiv e-prints, arXiv:1904.13286

Appendix A: Example of Sy1 and Sy2 spectra

The authors, in order to demonstrate that the final Sy1 sample consists of well-selected type 1 AGNs, present ten random Sy1 optical spectra (A.1), limited to $z < 0.2$, from the SDSS database. On the other hand, they comparatively present a sample of ten random Sy2 optical spectra (A.2) with redshifts up to $z = 0.2$.

